ASIA-PACIFIC JOURNAL OF CHEMICAL ENGINEERING
Asia-Pac. J. Chem. Eng. 2008; **3**: 151–160
Published online in Wiley InterScience
(www.interscience.wiley.com) DOI:10.1002/apj.127

Curtin University of Technology

Research Article

On the hydrodynamics of liquid–liquid slug flow capillary microreactors

M. N. Kashid,[1,2] D. Fernández Rivas,[3] D. W. Agar[2] and S. Turek[1]*

[1]*Institute for Applied Mathematics, University of Dortmund, Vogelpothsweg 87, 44227, Dortmund, Germany*
[2]*Institute of Reaction Engineering, University of Dortmund, Emil-Figge-Str., 66, 44227, Dortmund, Germany*
[3]*Departamento de Ingeniería Nuclear, Instituto Superior de Tecnología y Ciencias Aplicadas, InSTEC, Quinta de los Molinos, Ave. Salvador Allende y Luaces, Ciudad de la Habana, Cuba*

Received 28 February 2007; Revised 16 January 2008; Accepted 19 January 2008

ABSTRACT: Microreactor technology is an important method of process intensification. Liquid–liquid slug flow capillary microreactors have been used to intensify the reactions with heat and mass transfer limitations. In this type of reactor, either two liquids flow alternate to each other in a capillary or one liquid flows as a continuous flow while the other flows in the form of enclosed drops (slugs) depending on the interfacial tension between two liquids and liquid adhesion with the solid walls. The enhanced mass transfer is due to the internal circulations within the slugs, which rise due to the shearing action between the slug axis and the capillary wall or continuous phase. The slug size and the intensity of internal circulations depend on the type of mixing element and physical properties of the liquids. The proper understanding of physical behaviour of fluids at the microscale is a challenging issue for the growing microreactor application demands. This article highlights the hydrodynamic characteristics of the liquid–liquid slug flow capillary microreactor. Experimental results on flow regime, slug size and particle image velocimetry along with corresponding complementary state-of-the-art computational fluid dynamics (CFD) simulations are discussed in detail.

KEYWORDS: liquid–liquid slug flow; capillary microreactor; free-surface modelling; internal circulations; particle tracing

INTRODUCTION

Microreactor technology offers potential benefits to processing technology. Some of the benefits are minimal substances consumption, complex chemical waveforms and significantly reduced analysis or experiment time (e.g. an important concept recently introduced was μTAS, the Micro Total Analysis System, for details of which see Ref. 1). The absence of inertial and turbulent effects in microfluidic devices, due to the low ratio between the inertial forces and the viscous forces offers new horizons for physical, chemical and biological applications. Also, the short-length scales gives high surface-to-volume ratios, small diffusion distances and easy temperature profiling where needed, giving the opportunity to manipulate substances in a better and reliable way which provides every molecule the same processing experience. For large-scale production, the microreactors can be bundled together which reduces the risk associated with scale-up. The physical properties of liquids such as viscosity, surface tension and wall adhesion play a very important role at these small scales.

The liquid–liquid slug flow capillary microreactor concept was introduced for chemical engineering applications by Burns and Ramshaw[2] and has obtained mass transfer data for the extraction of acetic acid from kerosene slugs in a glass chip-based reactor and explained the performance of the system in terms of the prevailing slug lengths. Further, it has been used for different applications such as nitration reactions[3,4] and kinetic measurement in enzymatic reactions.[5] Dummann *et al*.[4] elucidated and optimised the nitration reaction and achieved significant reduction in by-product formation using a capillary microreactor compared to conventional process. Easy temperature profiling along the dimensions of the reactor allowed removing heat generated in the reaction, and low hold-up of the reactants guaranteed the safety during the reaction.

**Correspondence to*: M. N. Kashid, Institute for Applied Mathematics, University of Dortmund, Vogelpothsweg 87, 44227, Dortmund, Germany
Group of Catalytic Reaction Engineering (GGRC), Swiss Federal Institute of Technology (EPFL), CH-1015 Lausanne, Switzerland.
E-mail: Madhvanand.Kashid@epfl.ch;

The alternate flow can also be applied in modular synthetic chemistry, particularly in combinatorial chemistry so far as the reactants and products of the single synthesis steps are compatible with liquid–liquid two-phase systems.[6] Further reducing the size of the microreactor, this concept can be used for medical applications where nano-litre amounts of samples are involved. Such applications have already been published in the literature such as cell-based assays[7], models for capillary blood vessels for red cells infected with malaria[8], drug delivery targeted at specific sites in the body for a less invasive chemotherapy, miniature bio-sample preparations on fully automated bio-chips, for DNA sampling and other genomic applications.

Microreactor technology is a relatively new area and very few mathematical models have been developed to study hydrodynamics of two-phase flow (mostly gas–liquid) in small geometries. In one of our previous works,[9] we have carried out single-phase flow simulations to study the internal circulations, while in another study,[10] we carried out free-surface simulations to understand the mechanism of slug flow generation. In connection with this, there is a need to develop a numerical model which can give detailed information about the two-phase liquid–liquid flow in small channels, and complex flow in the vicinity of the interface which requires powerful modelling techniques. Mathematical models describing the movement of drops, or in general, multi-phase flows developed so far, are not able to predict or quantify properly all the important particularities of this complex system (capillary microreactors). Hence, a deeper knowledge of the physical problem, complex hydrodynamics in the vicinity of the interface between two slugs of liquid–liquid slug flow is mandatory. Different modelling approaches are available, but it is important to know the suitable model for the investigation of a particular parameter, and therefore, there is a need to have a short review on modelling approaches available for the study of drops/slug movement through capillaries, and this is what we present in this article.

In the present work, we discuss the hydrodynamic characteristics of the liquid–liquid slug flow capillary microreactor which were investigated using state-of-the-art experimental and computational techniques. The main focus of the article is on the movement of the interface, internal circulations within the slugs, and velocity patterns in the vicinity of the interface.

SLUG FLOW GENERATION AND CHARACTERISATION

Slug flow generation and flow regimes

The experimental set-up used to study the hydrodynamics of liquid–liquid slug flow is shown in Fig. 1. Two immiscible liquids (aqueous and organic from two reservoirs) were introduced by continuously operating high-precision piston pumps (throughput range of 1–999 ml/h) to a symmetric 120° Y-piece mixing element made of Teflon. Digital photos to investigate the flow regimes and slug size were taken using a commercial camera fitted at a distance of 0.5 m downstream of the mixing element and a light source (2000 W). Several combinations of Y-junction and capillary sizes were tested. In order to distinguish the two phases, the water phase was stained with a blue dye to appear darker than the colourless cyclohexane. The snapshots show that the water phase forms convex-shaped slugs, while cyclohexane exhibits a concave geometry as would be

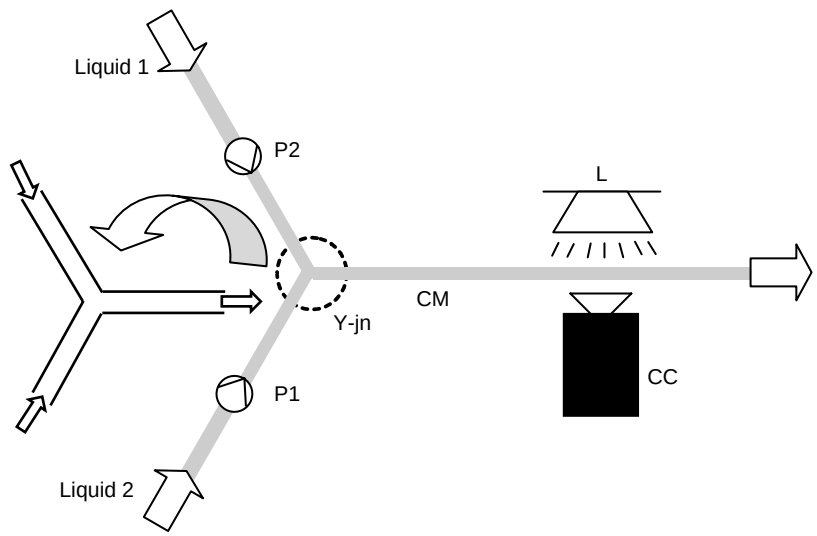

Figure 1. Experimental set-up: P1, P2 – pumps, Y-jn – Y-junction, CM – capillary microreactor, L – light and CC – camera.

DOI: 10.1002/apj

expected with the hydrophobic PTFE (polytetrafluoroethylene) wall material. The exact form of the slug depends on the inlet flow ratios, physical properties of both liquids, and the capillary and Y-junction dimensions.

The flow patterns in the capillary depend on several factors such as interfacial tension, wall adhesion and angle of contact between two liquid inlets at the Y-junction. When two immiscible liquids are introduced into the Y-junction, one liquid initially flows downstream through the junction, while the other penetrates over to the opposite side of the junction. This mutual displacement process generates the alternating slug flow structure. The flow regimes of two immiscible liquids in a capillary are defined on the behaviour of the aqueous phase in the two-phase flow. One can easily recognise three distinct flow regimes, well-defined slug flow, drop flow and deformed interface (inverted) flow which is explained in detail in Kashid and Agar.[11]

The slug size observed shows the influence of combination of different Y-junction and capillary dimensions. For a Y-junction with different capillaries, the slug size increases with increase in the capillary ID for all slug flow (Fig. 2) velocities. The same effect was observed with increased Y-junction diameters with the same capillary dimension–it yields larger slugs in comparison to smaller Y-junctions. An advantage of slug flow over parallel flow is that it can alter the interfacial area with change in the flow velocity–slug size decreases with an increase in the flow velocity and thus increases interfacial area. This is due to the rapid penetration of one phase into the other, which segregates the stream into a higher number of segments. An alternative method to change the interfacial area is to vary the ratio of inlet flow rates. In our experiments with variable flow rate ratios, which were carried out by keeping one liquid flow rate constant and varying the other, the volume of the slug phase with constant liquid flow rate decreases and the slug volume of a varying flow rate increases with an increase in the flow rate.

As mentioned before, due to superior wetting properties of one of the liquids with solid materials, a wall film formation takes place. In one of our previous studies on pressure drop in liquid–liquid slug flow capillary microreactor, it was revealed that cyclohexane forms an organic wall film with the PTFE capillary material.[11] In this case, the enclosed slug moves with relatively higher velocity than that of average slug flow velocity. The film thickness calculated by Bretherton's Law was in the range of 1–20 μm for all capillaries under the slug flow regime. Slug lengths were measured and film thickness calculated using Bretherton's Law was considered in the investigation of slug volume. The slug size as a function of superficial velocity of both phases for equal flow rates is plotted in Fig. 3(a). As expected, slug volume decreases with increase in the superficial velocity. It also shows no significant difference in the sizes of the slugs of both phases in the presence of a wall film. Experiments were also carried out for unequal flow rate of both phases by keeping one of the flow rates constant while varying the other. The results from Fig. 3(b) show that with an increase in the flow velocity of a particular phase, the slug size also increases, and vice versa. Thus, the slug size does not show any significant difference in the presence of a wall film.

CFD modelling

In immiscible liquids, the movement of interface is important in evaluating the performance of the reactor, and therefore, free-surface modelling is necessary. In the small-scale channels, the wall adhesion (interaction of liquid with solid wall) effects are dominant and they govern the flow patterns. Different methods are available to model immiscible fluids such as level set, volume of fluid (VOF), marker particle, Latice Boltzmann, front tracking and so on. A short review of these methods can be found in the work of van Sint Annaland *et al*.[12] VOF and level-set approaches belong to the most common implicit free-surface reconstruction methods, while, particularly, VOF is relatively simple to treat topological changes of the interface and is naturally conservative. This method was extensively used for many applications (e.g. Refs 13–16). This method solves the Navier-Stokes equations for velocity and pressure as given in the following equation:

$$\rho\left(\frac{\partial u}{\partial t} + (u.\nabla)u\right) = -\nabla p + \nabla \cdot \mu(\nabla u + \nabla u^T) + \rho g$$
$$\nabla \cdot u = 0 \tag{1}$$

where ρ and μ are the density and viscosity of liquids, respectively. The common interfacial boundary conditions, continuity of velocity across the interface and jump in the normal stresses are given by:

$$[u]|_\Gamma = 0, \quad -\left[-pI + \mu(\nabla u + \nabla u^T)\right]|_\Gamma \cdot \hat{n} = \sigma\kappa\hat{n} \tag{2}$$

Where σ is the surface tension, κ is the curvature of the interface and $\hat{n}$ is the normal vector to the surface interface (for more details see Ref. 17). The interface between two fluids is tracked by using a pure convection equation of the volume fraction of a phase.

$$\frac{\partial \alpha}{\partial t} + u.\nabla\alpha = 0 \tag{3}$$

The other method, the level-set method, solves similar types of equations. However, the interface is tracked by a function that is zero at the interface, positive in phase one and negative in the other. The evolution of this function can be posed as a general transport problem, i.e. convection equation similar to volume fraction in

DOI: 10.1002/apj

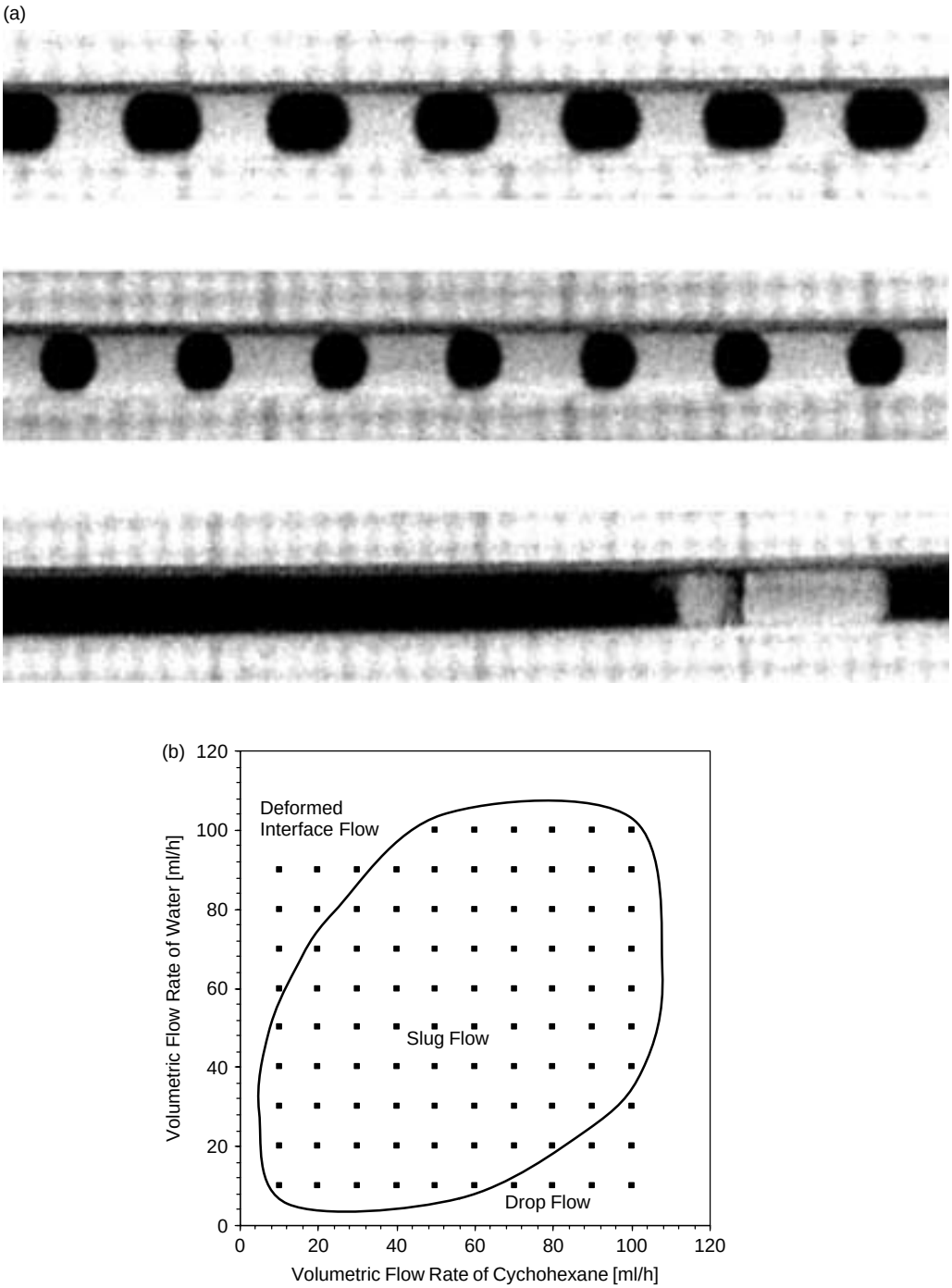

Figure 2. Flow regimes observed in the capillary microreactor (a) (i) slug flow, (ii) a drop flow and (iii) deformed interface flow; and (b) graphical representation for different volumetric flow rates. (Y-junction $ID = 1$ mm, Capillary $ID = 1$ mm).

the VOF method (Eqn (3)). As mentioned earlier in the liquid slug flow the flow patterns are governed by surface tension and wall adhesion forces and therefore the surface tension modelling is very crucial. It is usually done by using the continuum surface force (CSF) model proposed by Brackbill *et al*.[18] The addition of surface tension to the calculation results in a source term in the momentum equation.

In the liquid–liquid slug flow, if the surface tension between one of the liquid phases and the wall material is higher than the interfacial tension between two liquids, liquid flow in the form of an enclosed slug, while the other phase flow in the form of a continuous phase forming a thin wall film of a few micrometres in size. If the flow does not satisfy these conditions then both liquids flow alternatively. In this case, rather

DOI: 10.1002/apj

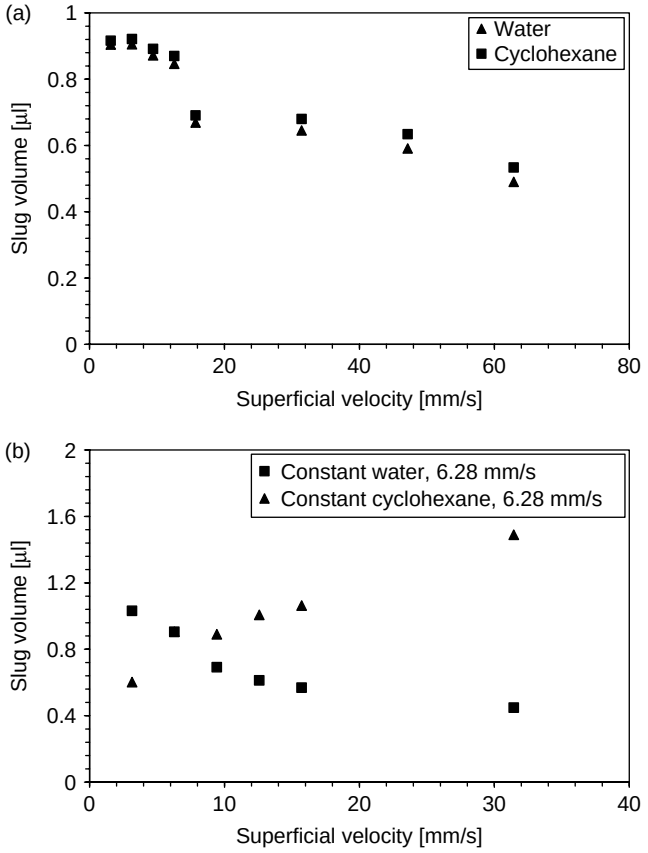

Figure 3. Slug volume as a function of superficial velocity for equal flow rate of both phases (capillary $ID = 0.75$ mm); (a) equal flow rates and (b) unequal flow rates.

than imposing the boundary conditions at the wall itself, the contact angle that the fluid assumed to make with the wall is used to adjust the surface normal in the cells near the wall. The contact angle values are taken from experimental measurements and no-slip boundary conditions (zero velocity on walls) are used. The liquid–liquid–solid contact line moves along the wall, presenting a kind of singularity.[19] In this case, the velocity of the faces adjacent to the wall is kept at zero, and the other parts (cell centre and other faces) have non-zero velocity. Such non-zero velocities influence the volume fraction field, and therefore, also the position of the interfaces. Thus, such implementation realises the movement of the liquid–liquid–solid contact line despite specifying no-slip boundary conditions at the solid surface. The simulated results using this methodology are depicted in Fig. 4(a). It shows well-defined slug flow for a three-phase contact angle of 90°.

Further, the 2D simulations were carried out using in-house-developed CFD code FEATFLOW. This code uses an implementation of surface tension effects in interfacial flow combining two techniques: the CSF method and a finite element discretisation together with the Laplace-Beltrami operator.[17] For the integration of the level-set function (interface between the slug and fluid around it), there are two different approaches at hand. On one hand, a specific number of cells are used for the integration of the level-set function, which makes possible the simple volume integration at a low computational cost, but less accurate. On the other hand, direct line integration technique is used in which the interface line is reconstructed exactly from where the surface tension forces are integrated, i.e. exactly on the lines, although it is computationally more expensive. For the time discretisation, a Crank-Nicholson scheme was used. The results obtained are plotted in Fig. 4(b). It also shows the well-defined slug flow. However, the back interface of the slug is deformed due to the lack of wall adhesion phenomenon, which is the subject of future work. The flow rate range in the study was 100 ml/h for all capillaries of diameter 0.5, 0.75 and 1 mm. The fine mesh size for all free-surface simulations was 0.001 times slug diameter (capillary diameter) and a time-step of $1-5 \times 10-5$ s was used.

INTERFACE BEHAVIOUR AND INTERNAL CIRCULATIONS

Particle image velocimetry

Particle imaging velocimetry (PIV) measurements were conducted to gain insight of the internal circulations within the slugs (Fig. 5). The images of the water (fluorescence) and paraffin oil system were recorded for PIV in a Caliper 42 Microfluidic Workstation, which uses microfluidic glass chip (LabChip NS145) with T-contactor to a capillary width of 70 µm and depth of 12 µm. The detailed experimental set-up is presented in Kashid *et al*.[9] The experimental PIV measurements were carried out at very low flow rates due to experimental limitations, while CFD simulations were carried out to study internal circulations over a wide operating window. The experimental snapshot of fluorescence particles with PIV investigations in terms of velocity vectors at an average flow velocity of 0.086 mm/s is shown in Fig. 5. From the experimental snapshots it is clear that part of the liquid in the vicinity of the slug walls shows the backflow, while the liquid in the middle of the slug shows flow in forward direction showing the internal circulations. Several videos recordings were taken sequentially during this experimental study, and it was observed that the wall film provides lubricating action to the enclosed slug, whereby the slug surrounded by film moves with higher speed as compared to the average velocity.

Free-surface modelling

Further, the level-set methodology presented in the above section is used to carry out simulations to study

DOI: 10.1002/apj

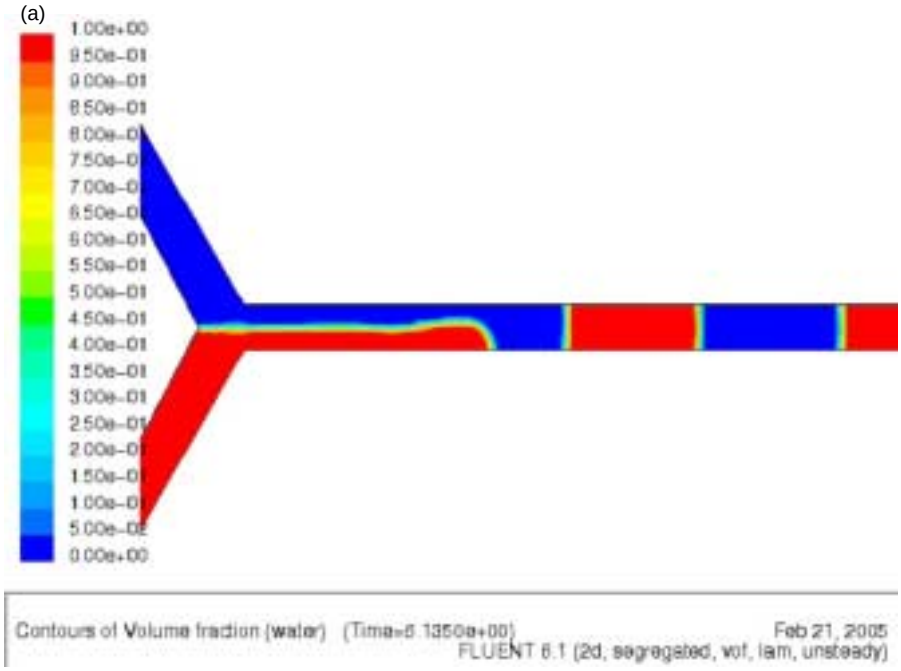

Volume of fluid method (u_1=10 mm/s, u_2=10 mm/s, θw = 90°) (using FLUENT, Kashid *et al.* 2007)

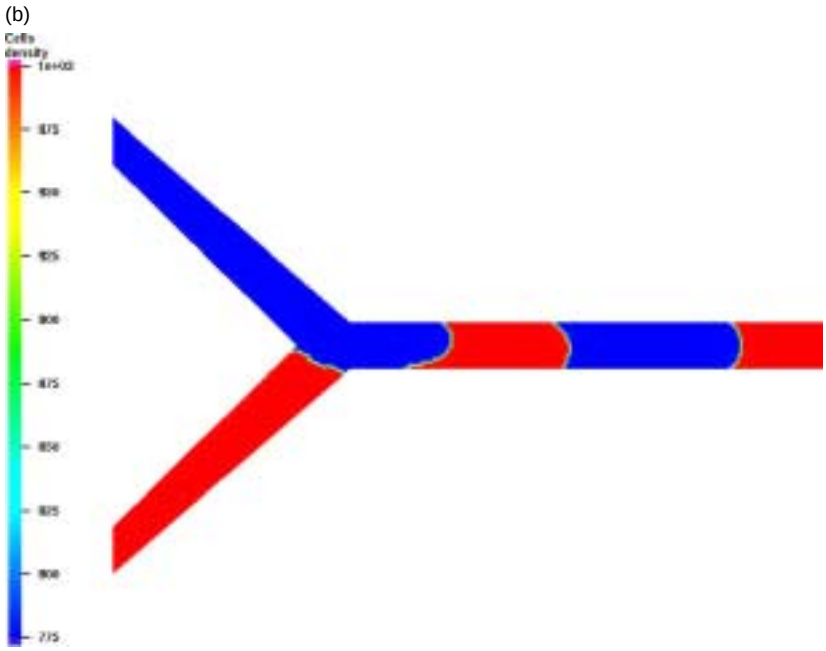

Figure 4. Simulated snapshot of the well-defined slug flow ($u_1 = 10$ mm/s, $u_2 = 10$ mm/s); (a) volume of fluid method and (b) level-set method. This figure is available in colour online at www.apjChemEng.com.

the interface behaviour and the flow patterns within the slugs of liquid–liquid slug flow. To follow flow patterns within the flowing slug in a capillary we have taken a long pipe and three slugs were placed as an initial condition as shown in Fig. 6(a). The physical properties of the liquids were defined corresponding to the properties of water–cyclohexane system, and the geometrical shapes of the slug were retrieved from the experimental snapshots. The parabolic profile was given at the inlet, and atmospheric pressure was defined at the outlet. The numerical mesh generated with the help of the in-house-developed Design and Visualisation Software Resource, and the level-set function defined to represent the interface is shown in Fig. 6(b). The simulations were carried out without wall adhesion effect.

DOI: 10.1002/apj

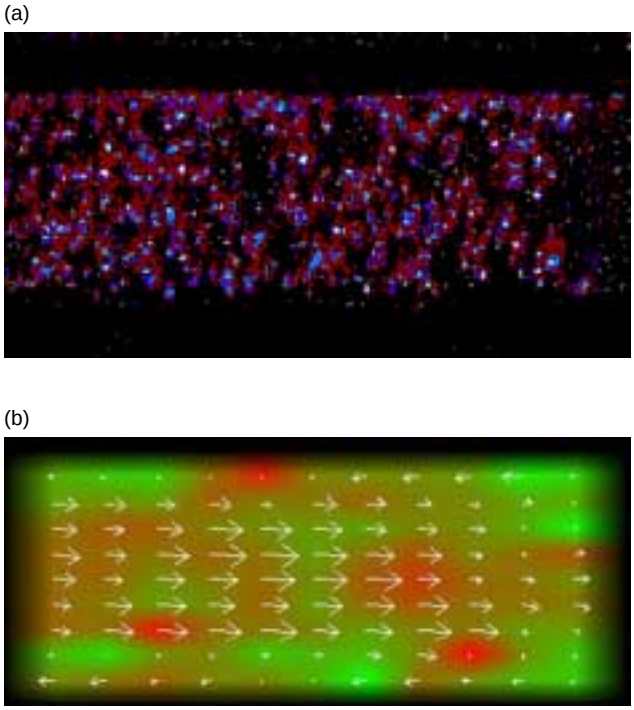

Figure 5. Internal circulation information from PIV measurements (Vav = 0.086 mm/s); (a) experimental snapshot, and (b) velocity distribution of PIV. This figure is available in colour online at www.apjChemEng.com.

The obtained results are plotted in Fig. 7. As can be seen from the Figure, the slug changes its shape considerably compared to the initial shape. Due to the shearing action between the slug axis and the continuous phase/wall axis each slug shows intense internal circulations. The closed look at the internal circulation within a slug shows the presence of stagnant zones. As can be seen in Fig. 7, there are four stagnation regions that can be identified within each slug on the upper and lower parts, and at the front and rear ends. In some slugs, the stagnant rear zone does appear if the rear side is a perfect hemisphere. Moving in a reference system with the slug's average velocity, the geometry of this configuration provides a symmetrical line along the axis of the capillary. The centre line of the slug flows in the direction of the slug's movement and is formed by the convergent streams of two eddies that separate at the nose, and then go in opposite directions to reunite at the tail. This internal convective movement is generated by the shear stress deformation acting on the interface of the slug and the carrier and can be also extrapolated to the internal movement of the carrier. In Fig. 7, the black colour stands for the minimum velocity (stagnant zone) and the white colour between the two lateral stagnant zones shows the maximum velocity. It was seen that increasing the average carrier velocity leads to an increase in the internal circulation within the slugs.

Particle tracing

When considering mass transfer and reactions in a microreactor, the transport of the species within the phases will be determined strongly by the hydrodynamic flow pattern. CFD particle tracing is a powerful flow-field visualisation tool that gives qualitative information about the flow patterns.

For the particle-tracing study we took one snapshot of the moving slug and considered it as stationary. This is done by subtracting the average velocity at which the slug is moving (from left to right in this case) to every node x-component value. Using the GMVPT

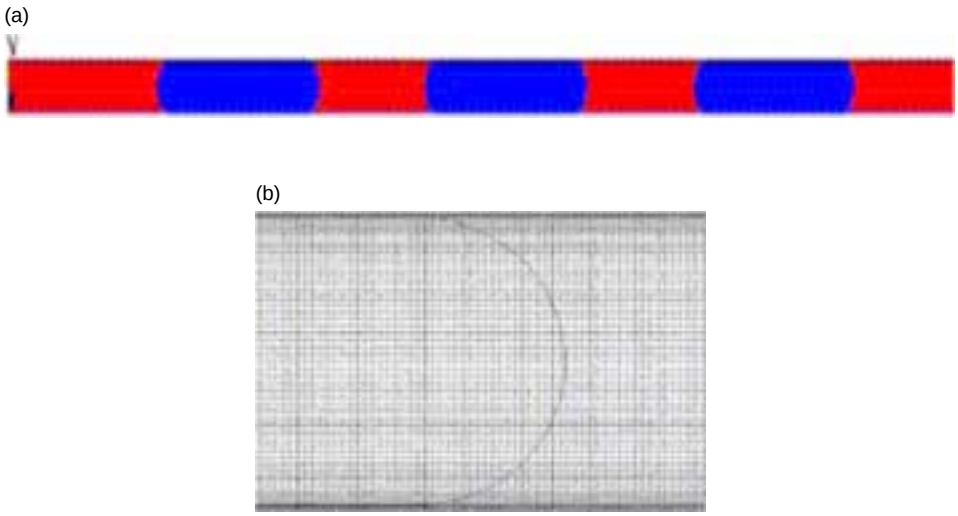

Figure 6. Initial conditions and numerical mesh; (a) initial shape of three slugs in a capillary, and (b) numerical mesh and initial interface shape. This figure is available in colour online at www.apjChemEng.com.

DOI: 10.1002/apj

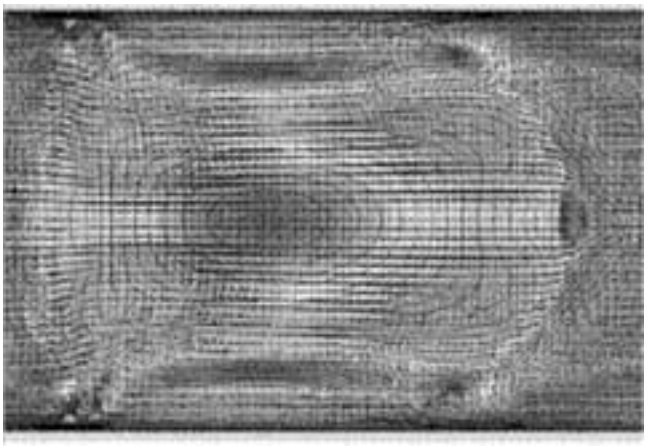

Figure 7. Internal circulations with slugs using free-surface modelling.

module (developed by FEATFLOW group, Institute for Applied Mathematics, University of Dortmund), initially a distribution of particles is placed in the back (left) part of the slug, and as the slug moves to the right (increasing the time-step), and the behaviour described above is exactly obtained (Fig. 8).

In the above figure it can be seen how the particles follow the centre stream and divide forming the two eddies referred to above. The stagnation zones are clearly spotted after a few time-steps. Comparing the particle-tracing numerical solution with the experimental PIV measurements, both results are, qualitatively speaking, the same and also coincide with the internal circulation expected flow pattern.

Simplified modelling–single phase

In the liquid–liquid slug flow, both liquids exert considerable shear on each other, and therefore, the flow patterns are very well defined (Fig. 9(a)). The above methodology, free-surface modelling, requires more computational resources, and therefore, the model can further be simplified assuming the fixed interface position retrieved from the experimental snapshots. The CFD simulations were carried out for each individual slugs and the re-circulation time and position of the stagnant zones was from the obtained data. Simulations were carried out for two cases: without film and with film. The length of the aqueous phase domain with and without film was assumed to be the same, while the radius was modified with film thickness for aqueous slug with film. For organic slugs without film, the domain was considered as a closed geometry, whereas with film there were inlet and outlet flows via the wall film. The front and rear interfaces of all slugs were assumed to be symmetric at all flow velocities even with the convective flow in or out of the organic slug via the film. The FEATFLOW was used for simulations which solves the following unsteady-state incompressible Navier-Stokes equation with velocity constraints by projected and coupled approach.[20]

$$\begin{aligned} &\frac{\partial u}{\partial t} + u.\nabla u - \nu \Delta u + \nabla p = f \\ &\nabla \cdot u = 0 \end{aligned} \tag{4}$$

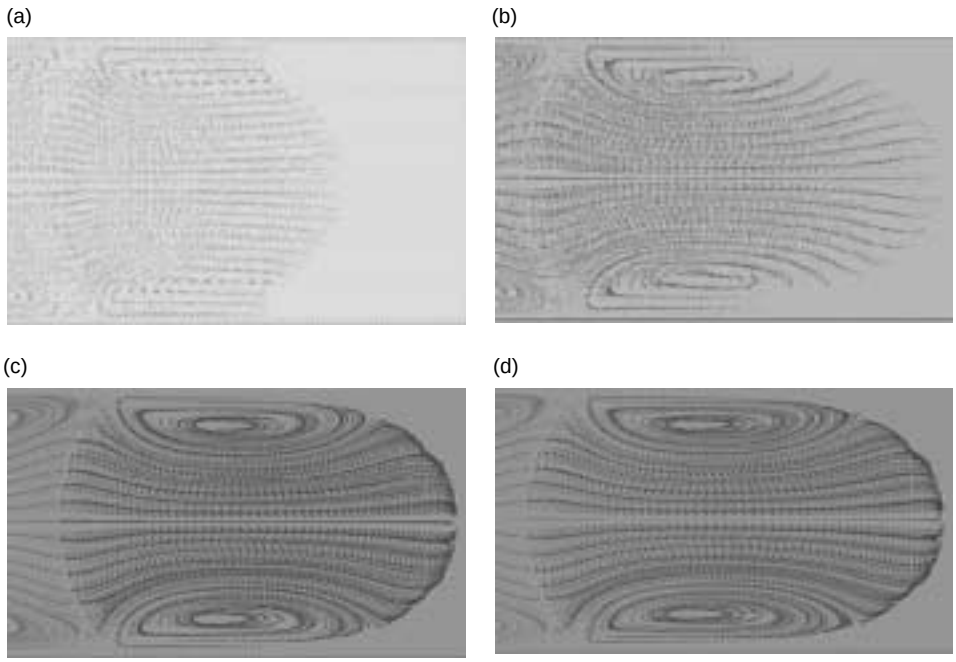

Figure 8. Particle-tracing evolution at different times inside a slug; (a) $T = 0.08$ s, (b) $T = 0.27$ s, (c) $T = 0.74$ s and (d) $T = 0.97$ s.

DOI: 10.1002/apj

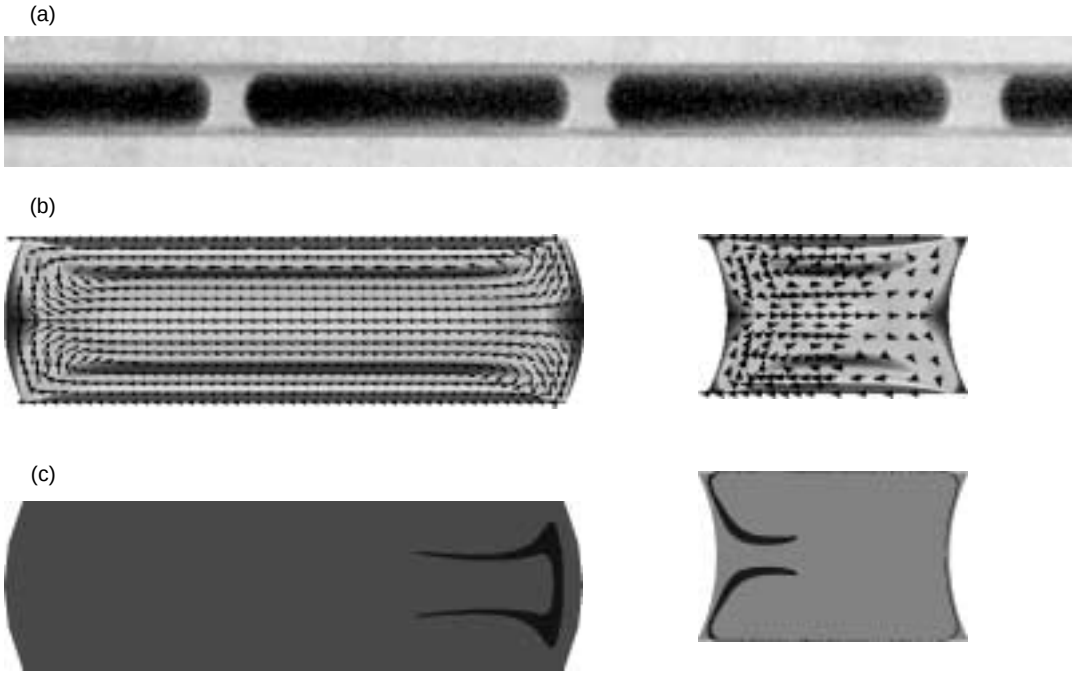

Figure 9. (a) Snapshots of CFD simulations and particle tracing using simplified CFD simulations for internal circulations; (b) CFD simulations; and (c) particle tracing (Vav = 5.64 mm/s, $D = 0.75$ mm).

The structured two-dimensional coarse grid was generated and was refined near the wall and corner of the geometry to improve the resolution. The Dirichlet-type boundary conditions were used for the aqueous slug with and without film. The same boundary conditions were used for the organic slug without film as there was no inflow and outflow. For organic phase domain with film, i.e. with film inlet and outlet flows, Neumann-type boundary conditions were used. A negative x-velocity was given to the capillary wall, which moved the capillary wall in a negative direction while the slug remained stationary. The other parameters were defined relative to the slug velocity according to domain requirement.

Further, the simulations for particle tracing were carried out with the result obtained from CFD simulations. The meshes with different levels of refinement were generated with the help of the in-house-developed graphical pre-processing tool, TRIGEN2D, a tool for two-dimensional coarse triangulations, and to write the corresponding data in special format onto a hard disc. A rectangular area of tracers was defined with a constant frequency to simulate a constant stream of particles at various operating conditions. The obtained results are plotted in Fig. 9(b) and (c). As can be seen from the figure, the liquid in the centre part of the slug moves towards the front interface while the liquid in the vicinity of the wall moves in the backward direction showing intense internal circulations.

CONCLUSIONS

In this article, the experimental and simulation results on the slug flow generation, flow patterns, interface movement and fluid flow within the slugs (internal circulations) are presented. Three flow regimes, slug flow, drop flow and deformed interface flow were observed in the capillary microreactor. The methodology presented for the slug flow can capture slug flow generation which shows that the processes relevant to the liquid–liquid slug flow capillary microreactor can be studied numerically. Further, the interface movement and internal circulations using single-phase and two-phase simulations showed very good results for the flow patterns and stagnation zones within the slugs which is very important to predict the mixing within the slugs. The presented numerical models can be tested under different flow conditions and fluid properties, being a versatile tool for the design of capillary microreactors.

Acknowledgement

The authors acknowledge the help of Mr. Shuren Hysing in performing the levelset simulations described.

REFERENCES

[1] A. Manz, N. Graber, H.M. Widmer. *Sens. Actuators*, **1990; *B1*,** 244–248.

[2] J.R. Burns, C. Ramshaw. *Lab. Chip.*, **2001;** *1*, 10–15.
[3] J.R. Burns, C. Ramshaw. *Chem. Eng. Commun.*, **2002;** *189*, 1611–1628.
[4] G. Dummann, U. Quittmann, L. Groschel, D.W. Agar, O. Woerz, K. Morgenschweis. *Catal. Today*, **2003;** *79–80*, 433–439.
[5] H. Song, R.F. Ismagilov. *J. Am. Chem. Soc.*, **2003;** *125*, 14613–14619.
[6] J.M. Koehler, T.h. Henkel, A. Grodrian, T.h. Kirner, M. Roth, K. Martin, J. Metze. *Chem. Eng. J.*, **2004;** *101*, 201–216.
[7] J. Pihl, J. Sinclair, M. Karlsson, O. Orwar. *Mater. Today*, **2005;** *8*, 46–51.
[8] J.P. Shelby, J. White, K. Ganesan, P.K. Rathod, D.T. Chiu. *Proc. Natl. Acad. Sci. U.S.A.*, **2003;** *100*, 14618–14622.
[9] M.N. Kashid, I. Garlach, S. Goetz, J. Franzke, J.F. Acker, F. Platte, D.W. Agar, S. Turek. *Ind. Eng. Chem. Res.*, **2005;** *44*, 5003–5010.
[10] M.N. Kashid, F. Platte, D.W. Agar, S. Turek. *J. Comput. Appl. Math.*, **2007;** *203*, 487–497.
[11] M.N. Kashid, D.W. Agar. *Chem. Eng. J.*, **2007;** *131*, 1–13.
[12] M. van Sint Annaland, W. Dijkhuizen, N.G. Deen, J.A.M. Kuipers. *AIChE J.*, **2006;** *52*, 99–110.
[13] D. Bothe, M. Koebe, K. Wielage, H-J. Warnecke. VOF simulations of mass transfer from single bubbles and bubble chains rising in the aqueous solutions. In *Proceedings of FEDSM03: Fourth ASME-JSME Joint Fluids Engineering Conference*, Honolulu, July 6–11, **2003**.
[14] G. Cerne, S. Petelin, I. Tiselj. *J. Comput. Phys.*, **2001;** *171*, 776–804.
[15] L. Chen, Y. Li. *Environ. Model. Softw.*, **1998;** *13*, 247–255.
[16] J. Li, Y. Renardy. *Soc. Ind. Appl. Math.*, **2000;** *42*, 417–439.
[17] S. Hysing. *Int. J. Numer. Methods Fluids*, **2006;** *51*, 659–672.
[18] J.U. Brackbill, D.B. Kothe, C. Zemach. *J. Comput. Phys.*, **1992;** *100*, 335–354.
[19] P.R. Gunjal. Flow modeling and mixing in packed bed reactor, PhD Thesis, IIT, Mumbai, **2005**.
[20] S. Turek. *Efficient Solvers for Incompressible Flow Problems: An Algorithmic and Computational Approach*, Springer-Verlag: Heidelberg, **1999**.